Ultrafine Platinum Nanoparticles Uniformly Dispersed on Arrayed CN_x Nanotubes with High Electrochemical Activity

Chia-Liang Sun,[†,‡] Li-Chyong Chen,*[,‡] Ming-Chuan Su,[§] Lu-Sheng Hong,[§] Oliver Chyan,[||] Chien-Yu Hsu,[†] Kuei-Hsien Chen,[†] Te-Fu Chang,[⊥] and Li Chang[⊥]

Institute of Atomic and Molecular Sciences, Academia Sinica, P.O. Box 23-166, Center for Condensed Matter Sciences, National Taiwan University, and Department of Chemical Engineering, National Taiwan University of Science and Technology, Taipei, Taiwan, Department of Chemistry, University of North Texas, Denton, Texas 76203, and Department of Materials Science and Engineering, National Chiao Tung University, Hsinchu, Taiwan

Received January 18, 2005. Revised Manuscript Received April 21, 2005

The structure and electrochemical properties of arrayed nitrogen-containing carbon nanotube (CN_x NT)−platinum nanoparticle (Pt NP) composites directly grown on Si substrates have been investigated. The CN_x nanotube arrays were grown by microwave-plasma-enhanced chemical vapor deposition first and then acted as the template and support for Pt dispersion in the following sputtering process. Under the same sputtering conditions, it was found that well-separated Pt NPs would form with an average diameter of 2 nm on the arrayed NTs while a continuous Pt thin film was observed on the bare Si substrate. X-ray photoelectron spectroscopy (XPS), X-ray diffraction, and electron microscopy were employed to study bonding and structure changes with increasing deposition time. Implications of the C1s and N1s bonding changes in XPS and their possible relation to the NT−Pt composite structures with self-limited size distribution are discussed. Cyclic voltammograms show well-behaved curves in methanol oxidation, suggesting an efficient electronic conduction mechanism from the substrate via CN_x NTs to reach individual Pt NPs is in operation. Such an integrated nanocomposite approach possesses a high potential for micro direct methanol fuel cell applications.

Introduction

Hybrid nanocomposites containing various kinds of nanomaterials are becoming more and more important as different functions from each constituent component are required for some demanding applications. Using one-dimensional (1D) nanomaterials, such as nanotubes and nanowires, as the basic building blocks, various classes of nanocomposites have been derived. The first class of the 1D nanocomposites has at least two 1D nanocomponents connected either sequentially in a line or in the form of coaxial nanocables.[1−5] The second class of the hybrid 1D nanocomposites is constituted of both 1D and zero-dimensional (0D) nanomaterials, such as quantum dots and nanoparticles (NPs). If a chain of NPs are encapsulated inside the 1D nanomaterials, the so-called nanopeapods are formed.[6−9] Alternatively, the NPs can be attached on the sidewalls of 1D nanomaterials. For example, carbon nanotubes (CNTs) have been exploited as the support for NPs which are made by the chemical solution method using metal organic precursors.[10−12] However, besides complicated template construction and removal in this method, special chemicals are always required to modify either the surface of CNTs or that of NPs. Although Zhang and coworkers have synthesized metal nanowires on suspended CNT by electron-beam evaporation,[13,14] there is little information available on arrayed nanocomposites following this method.

* To whom correspondence should be addressed. Phone: 886-2-33665249. Fax: 886-2-23655404. E-mail: chenlc@ccms.ntu.edu.tw.
[†] Academia Sinica.
[‡] National Taiwan University.
[§] National Taiwan University of Science and Technology.
[||] University of North Texas.
[⊥] National Chiao Tung University.

(1) Ajayan, P. M.; Iijima, S. *Nature* **1993**, *361*, 333−334.
(2) Lauhon, L. J.; Gudiksen, M. S.; Wang, D.; Lieber, C. M. *Nature* **2002**, *420*, 57−61.
(3) Lin, H. M.; Chen, Y. L.; Yang, J.; Liu, Y. C.; Yin, K. M.; Kai, J. J.; Chen, F. R.; Chen, L. C.; Chen, Y. F.; Chen, C. C. *Nano Lett.* **2003**, *3*, 537−541.
(4) Hu, J.; Bando, Y.; Liu, Z. *Adv. Mater.* **2003**, *15*, 1000−1003.
(5) Meng, X. M.; Hu, J. Q.; Jiang, Y.; Lee, C. S.; Lee, S. T. *Appl. Phys. Lett.* **2003**, *83*, 2241−2243.
(6) Smith, B. W.; Monthioux, M.; Luzzi, D. E. *Nature* **1998**, *396*, 323−324.
(7) Suenaga, K.; Tence, T.; Mory, C.; Colliex, C.; Kato, H.; Okazaki, T.; Shinohara, H.; Hirahara, K.; Bandow, S.; Iijima, S. *Science* **2000**, *290*, 2280−2283.
(8) Wu, J. S.; Dhara, S.; Wu, C. T.; Chen, K. H.; Chen, Y. F.; Chen, L. C. *Adv. Mater.* **2002**, *14*, 1847−1850.
(9) Hernández, E.; Menuier, V.; Smith, B. W.; Rurali, R.; Terrones, H.; Nardeli, M. B.; Terrones, M.; Luzzi, D. E.; Charlier, J. C. *Nano Lett.* **2003**, *3*, 1037−1042.
(10) Che, G.; Lakshmi, B. B.; Fisher, E. R.; Martin, C. R. *Nature* **1998**, *393*, 346−349.
(11) Jiang, K.; Eitan, A.; Schadler, L. S.; Ajayan, P. M.; Siegel, R. W.; Grobert, N.; Mayne, M.; Reyes-Reyes, M.; Terrones, H.; Terrones, M. *Nano Lett.* **2003**, *3*, 275−277.
(12) Endo, M.; Kim, Y. A.; Ezaka, M.; Osada, K.; Yanagisawa, T.; Hayashi, T.; Terrones, M.; Dresselhaus, M. S. *Nano Lett.* **2003**, *3*, 723−726.
(13) Zhang, Y.; Franklin, N. W.; Chen, R. J.; Dai, H. *Chem. Phys. Lett.* **2000**, *77*, 35−41.
(14) Kong, J.; Chapline, M. G.; Dai, H. *Adv. Mater.* **2000**, *18*, 1384−1386.

10.1021/cm050107r CCC: $30.25
Published on Web 06/08/2005

It has been recognized that precise control of nanomaterials and subsequent integration with the mainstream Si technology will be playing a crucial role in the future development of nanotechnology. A remarkable example is the site-specific or patterened growth of aligned CNTs on a Si wafer with good length control, which enables a wide range of CNT-based devices, such as gate-controlled and thin-film-transistor-controlled field emission devices.[15−19] Furthermore, CNTs can serve as the active part of Si devices after functionalization.[20−22] However, few studies have been done on the utilization of arrayed nanocomposites directly on silicon (Si) wafer substrates for electrochemical microsystems.[23] In this paper, we report an efficient and simple route to prepare nanocomposites with platinum NPs on a vertically aligned nitrogen-containing carbon nanotube (CN_x NT) array on Si substrates. Uniform Pt NPs, ca. 2 nm in average diameter, can be formed around the sidewalls of CN_x NTs over a large area using the simple sputtering method without any wet chemical pretreatments or the use of metal organic precursors. X-ray photoelectron spectroscopy (XPS) data reveal that the bonding between C and N of CN_x NTs may have been affected by Pt sputter deposition. Furthermore, electrochemical investigation suggests Pt NPs are electronically accessible through CN_x NTs and they exhibit favorable electron-transfer properties with H_2 production and methanol (CH_3OH) oxidation. The latter finding is especially interesting in the context of the bipolar plate application in the micro direct methanol fuel cell (μDMFC) devices.[24]

Experimental Section

For CN_x NT array preparation, an iron thin film was deposited on Si substrates by ion beam evaporation as catalysts prior to the NT growth step. Then aligned CN_x NTs were grown on the precoated substrates by microwave-plasma-enhanced chemical vapor deposition (MPECVD). The MPECVD growth was performed with the microwave power at 2 kW, mixtures of CH_4, N_2, and H_2 as source gases, and a substrate temperature of 1000 °C. Other details for the NT array growth process are described in our previous paper.[19] For Pt deposition, DC sputtering under Ar gas flow was performed and the deposition time was controlled between 1 and 15 min. Two kinds of substrates, namely, bare Si and CN_x NT-covered Si (CN_x NTs/Si), were compared in this study.

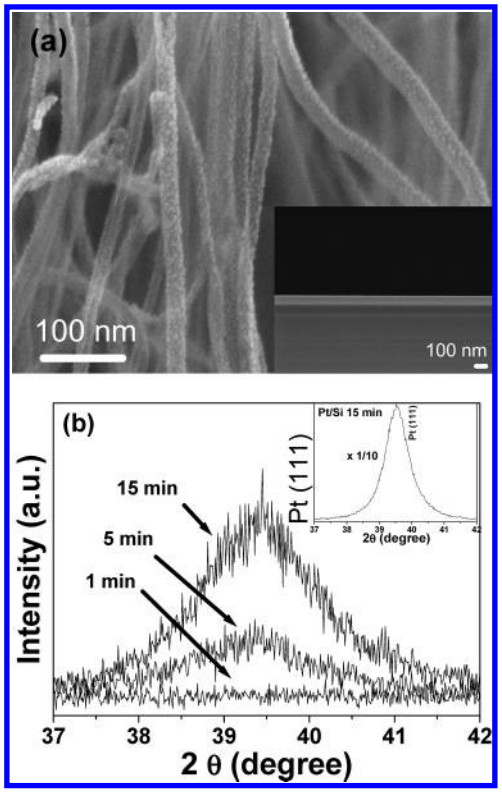

Figure 1. (a) Cross-sectional SEM image of Pt NPs on a CN_x NT/Si substrate after 15 min of deposition. The inset is that of a Pt thin film on a Si substrate. (b) XRD patterns of Pt NPs on a CN_x NT/Si substrate with different deposition times. The inset is that of a Pt thin film on a Si substrate after 15 min of deposition.

For material analyses, a Rigaku X-ray diffractometer and a JEOL 6700 field-emission scanning electron microscope were used. In addition, the products on the NT/Si substrate were scratched and dispersed on a lacey-carbon-covered Cu grid for transmission electron microscopy (TEM) (Philips Tecnai 20) observation. Moreover, XPS (VG Scientific ESCALAB 250) was used to study the composition and bonding change. Cyclic voltammograms were measured by using an Autolab potentiostat system.

Results and Discussion

Figure 1a illustrates the cross-sectional scanning electron microscopy (SEM) image of the CN_x NT/Si substrate after deposition of Pt for 15 min. The diameters of single NTs ranged from 13 to 33 nm as determined directly from the SEM micrograph. Uniformly distributed nanoclusters are clearly observed on the sidewalls of arrayed NTs, though it is difficult to determine their actual sizes due to the resolution limit of SEM. In contrast, as shown in the inset in Figure 1a, Pt forms a continuous thin film of about 90 nm in thickness on bare Si under the same conditions. Figure 1b shows the X-ray diffraction (XRD) patterns of Pt deposited on NT/Si substrates prepared with different deposition times. No obvious peak can be detected below a 5 min deposition time, and the small sizes of Pt nanoclusters observed are further confirmed by the broad and weak peaks at Pt(111) (Figure 1b).

Figure 2a displays the typical TEM micrograph of s single Pt-coated NT with a tube diameter of about 27 nm. The bamboo-like structure of the NT is a characteristic feature of nitrogen-containing NTs and, accompanying the high

(15) Cheng, H. C.; Hong, W. K.; Tarntair, F. G.; Lin, J. B.; Chen, K. H.; Chen, L. C. *Electrochem. Solid State Lett.* **2001**, *4* (4), H5−H7.
(16) Cheng, H. C.; Chen, K. J.; Hong, W. K.; Tarntair, F. G.; Lin, J. B.; Chen, K. H.; Chen, L. C. *Electrochem. Solid State Lett.* **2001**, *4* (8), H15−H17.
(17) Hong, W. K.; Chen, K. H.; Chen, L. C.; Tarntair, F. G.; Chen, K. J.; Lin, J. B.; Cheng, H. C. *Jpn J. Appl. Phys.* **2001**, *40* (5A), 3468−3473.
(18) Chen, L. C.; Hong, W. K.; Tarntair, F. G.; Chen, K. J.; Lin, J. B.; Kichambare, P. D.; Cheng, H. C.; Chen, K. H. *New Diamond Front. Carbon Technol.* **2001**, *11*, 249−263.
(19) Chen, L. C.; Wen, C. Y.; Liang, C. H.; Hong, W. K.; Chen, K. J.; Cheng, H. C.; Shen, C.S.; Wu, C. T.; Chen, K. H. *Adv. Funct. Mater.* **2002**, *12*, 687−692.
(20) Ravindran, S.; Chaudhary, S.; Colburn, B.; Ozkan, M.; Ozkan, C. S. *Nano Lett.* **2003**, *3*, 447−453.
(21) Balasubramanian, K.; Friedrich, M.; Jiang, C.; Fan, Y.; Mews, A.; Burghard, M.; Kern, K. *Adv. Mater.* **2003**, *15*, 1515−1518.
(22) Long, D. P.; Lazorcik, J. L.; Shashidhar, R. *Adv. Mater.* **2004**, *16*, 814−818.
(23) Ehrfeld, W. *Electrochim. Acta* **2003**, *48*, 2857−2868.
(24) Lu, G. Q.; Wang, C. Y.; Yen, T. J.; Zhang, X. *Electrochim. Acta* **2004**, *49*, 821−828.

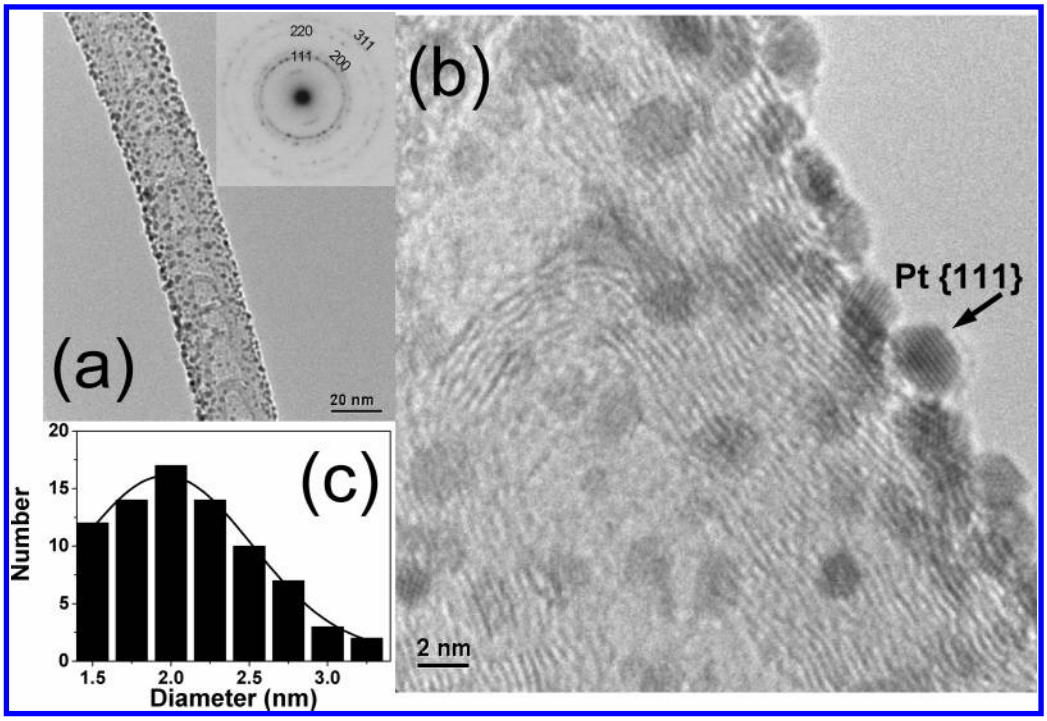

Figure 2. (a) TEM image of Pt NPs on the sidewall of one single CN_x NT with the corresponding SAED pattern in the inset. (b) HRTEM image of Pt NPs on the sidewall of one single CN_x NT. (c) A size histogram of Pt NPs estimated from (b).

density of the NTs, also results in the vertical array formation.[19] It is quite clear that the Pt nanoclusters formed on the sidewall of the NT are well-separated. Also shown in the inset of Figure 2a is the corresponding selected area electron diffraction (SAED) pattern of this Pt-coated NT, the ring pattern of which indicated these Pt NPs were randomly oriented. A high-resolution transmission electron microscopy (HRTEM) picture with a higher magnification of the same NT is also shown in Figure 2b. As indicated by the arrow in Figure 2b, a clear lattice fringe of Pt with the particle size as small as 2 nm can be observed. It should be noted that this arrow indicates the {111} planes of this Pt NP. The diameter of an individual Pt NP was analyzed from the HRTEM picture, and the resultant size histogram is shown in Figure 2c. The average diameter of these NPs can be estimated to be about 2 nm by Gaussian fitting.

Figure 3 shows the XPS C1s and N1s spectra of CN_x NTs before and after Pt coating, respectively. In all the C1s spectra (Figure 3a), the main peak located at about 285 eV is attributed to the sp^2-hybridized carbon bonds from the graphite layer of NTs.[25] For the uncoated CN_x NTs, a noticeable broad peak (as indicated by an arrow) is also observed in the high-binding-energy region, which can be attributed to the C and N bonding due to the N incorporation in NTs. When the deposition time was increased, it was found that this high-binding-energy C peak became progressively weaker and disappeared eventually. The corresponding N1s spectra are shown in Figure 3b, confirming that the N content does decrease with increasing deposition time. This could be attributed to the energetic particle bombardment as well as the block effect of Pt particles. It should be noted that there are two peaks in the N1s spectra. The one denoted as I_G in the high-binding-energy side (~400.3 eV) is the feature of N bonding in the graphite layer of the NT wall, and the other one denoted as I_P in the low-binding-energy side corresponds to the pyridine-type N bonding which causes the interlinked node morphology inside the CN_x NTs.[26] Comparing a series of spectra of these two peaks before and after Pt deposition, the integrated area ratio of I_G to the total of the two peaks decreased with increasing deposition time, suggesting that the reduction in the N peak of the graphite layer (I_G) was faster than that of the pyridine type (I_P). These XPS data implied that the graphite layer in the outer shell of CN_x NTs would be affected much easier by Pt NPs than the inner node.

Figure 4 displays a schematic diagram for the formation of arrayed nanocomposites. The column in the left-hand side is one single CN_x NT with the bamboo structure, in which the striped part labeled as G is the graphite layers with substitution-type nitrogen and the gray part labeled as P is the crossed node with pyridine-type nitrogen. Corroborated by the XPS analyses shown above, the Pt NPs would be most readily attached on the sidewalls of NTs at first and only very few of them may get into the node while a large amount of NPs progressively covered the sidewalls as the deposition time increased. Furthermore, it is found that the morphologies also depend on the vertical positions along the NTs. Namely, there are more Pt NPs on the top portions of NTs than the bottom at the same deposition time. With

(25) Ago, H.; Kugler, T.; Cacialli, F.; Salaneck, W. R.; Shaffer, M. S. P.; Windle, A. H.; Friend, R. H. *J. Phys. Chem. B* **1999**, *103*, 8116−8121.

(26) Terrones, M.; Ajayan, P. M.; Banhart, F.; Blase, X.; Carroll, D. L.; Charlier, J. C.; Czerw, R.; Foley, B.; Grobert, N.; Kamalakaran, R.; Kohler-Redlich, P.; Rühle, M.; Seeger, T.; Terrones, H. *Appl. Phys. A* **2002,** *74*, 355−361.

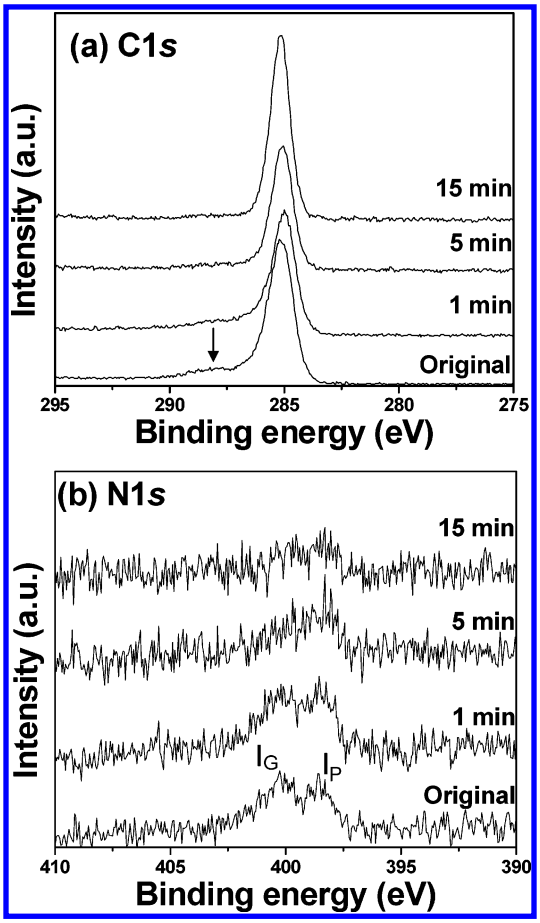

Figure 3. Evolution of XPS (a) C1s and (b) N1s spectra of arrayed CN_x NTs before and after Pt deposition from 1 to 15 min.

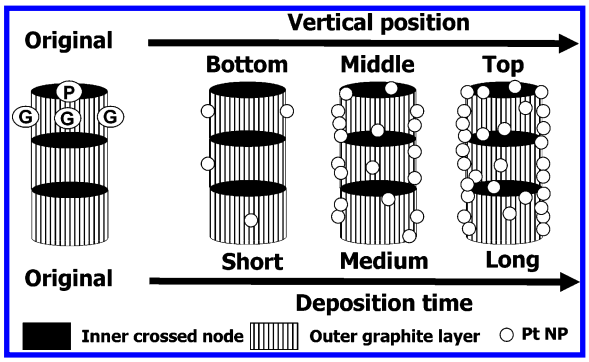

Figure 4. Schematic diagram for the formation of nanocomposites showing the morphology as a function of the deposition time at a fixed vertical position on CN_x NTs, or with respect to the different vertical positions at a fixed deposition time. The original CN_x NTs have two types of N bondings labeled with G and P, respectively.

increasing deposition time, the XRD peak (Figure 1b) showed increasing intensity but almost the same full width at half-maximum (fwhm) value, indicating that these Pt NPs, while increased in total number, could maintain a similar size distribution. Thus, we conjectured a self-limited growth of Pt NPs, presumably due to the fact that the sputtered Pt atoms were confined by the capture sites, among which the substitutional nitrogen sites might provide the main initial nucleation sites for the formation of Pt NPs.[11,12]

The cyclic voltammetry (CV) curves in Figure 5 show the electrochemical properties in different electrolytes of arrayed nanocomposites directly grown on conductive n^+-type Si

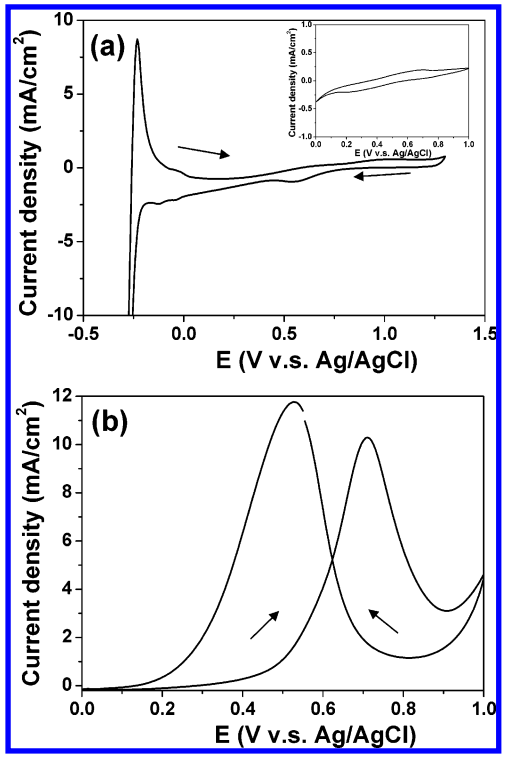

Figure 5. (a) Typical CV curve of the arrayed CN_x NT/Pt NP nanocomposites (15 min deposition) at a scan rate of 50 mV/s (1 M H_2SO_4). The inset shows the CV curve of CN_x NTs before deposition. (b) Corresponding CV curve of nominally the same arrayed CN_x NT/Pt NP nanocomposites (15 min of deposition) measured at the same scan rate of 50 mV/s but in 1 M CH_3OH/1 M H_2SO_4 solution.

substrates. Figure 5a displays a typical CV curve measured in 1 M H_2SO_4 for the arrayed CN_x NT/Pt NP nanocomposites. In contrast to the CV curve measured without Pt coating in the inset, the as-prepared Pt NPs supported by CN_x NTs show enhanced electron-transfer kinetics for the hydrogen evolution process, as evidenced by two distinct hydride absorption peaks (ca. −0.05 and −0.1 V vs Ag/AgCl) prior to the massive hydrogen evolution cathodic peak at −0.25 V. The CV results demonstrate that an efficient electronic conduction mechanism from the substrate via CN_x NTs to reach individual Pt NPs is in operation. Furthermore, Figure 5b illustrates a CV curve obtained from the CN_x NT/Pt NP nanocomposite electrode in 1 M CH_3OH/1 M H_2SO_4 solution. The characteristic methanol oxidation peaks were found for NT/Pt nanocmoposites, indicating that the new nanocomposites can have useful catalytic applications in the μDMFC.[10,23]

Conclusion

In summary, we have demonstrated an efficient and simple route to prepare arrayed NT/Pt NP nanocomposites by the combination of MPECVD and sputtering methods. With the same deposition parameters, it was found that Pt formed a thin film on the bare Si substrate but isolated NPs with an average diameter of 2 nm on the NT-covered Si. The different morphologies of these two cases could be originated from the different surface areas and interface energies of these two kinds of substrates. The nitrogen incorporation in the carbon nanotubes may also play some role in the self-

limited growth of the Pt NPs. XPS spectra revealed that the N content of the NTs progressively decreased after Pt sputtering. Analysis of the split peaks in N1s spectra as a function of deposition time corroborates the X-ray diffraction and electron microscopy studies to show that the Pt NPs will form predominantly on the graphite layers of the outer NT walls. The CV curves of arrayed nanocomposites demonstrate that the large-scale and fine Pt NPs supported by arrayed CN_x NTs are indeed electrochemically active and thus promising for a future μDMFC device.

Acknowledgment. We acknowledge the support by the National Science Council and Ministry of Education in Taiwan. O.C. thanks the Robert A. Welch Foundation for support. C.L.S. thanks the Instrumentation Center of National Taiwan University for the XPS measurement.

CM050107R